

Prediction of Henry's Constants for Alkane/Alkane Binaries above Solute Critical

Satoru Kato

Dept. of Applied Chemistry, Graduate School of Engineering, Tokyo Metropolitan University, 1-1, Minamiohsawa, Hachiohji 192-0397, Japan

DOI 10.1002/aic.10570

Published online August 19, 2005 in Wiley InterScience (www.interscience.wiley.com).

A universal prediction method for Henry's constants of alkanes in alkane solvents has not been established. The present study proposes a universal method for the prediction of Henry's constants representing all of the data for alkane/alkane binaries in the literature. The method involves two universal constants and works at $T_{ri} < 3$, where T_{ri} denotes the reduced temperatures of the solute alkanes. One of the constants modifies the expression of the infinite-dilution activity coefficients for their application to simple fluids reflecting end-to-sphere molecular orientations, whereas the other represents the vapor pressures of hypothetical liquids defined above solute critical. The prediction method also satisfactorily predicts the Henry's constants of rare gases and liquids having spherical molecules, such as Ar, Kr, Xe, and CCl_4 , in alkane solvents. Using the prediction method, the most reliable data of high-pressure vapor–liquid equilibrium for alkane/alkane binaries under dilute conditions in the literature were identified. © 2005 American Institute of Chemical Engineers AIChE J, 51: 3275–3285, 2005

Keywords: Henry's law constants, alkanes, infinite-dilution activity coefficients, simple fluids, hypothetical liquids

Introduction

Henry's law constants are of practical importance for the rational design of separation devices in the petroleum and petrochemical industries. Henry's law constants of an alkane solute i (H_i^∞) and the infinite-dilution activity coefficients of solute i (γ_i^∞), dissolved in alkane solvents, are of profound theoretical interest in thermodynamics because it is an important simplicity that the dispersion force is the only attractive molecular interaction acting on the alkane molecules. On the basis of these insights, a great number of experimental data for H_i^∞ in alkane/alkane binaries have been reported in the literature. However, at present, a method predicting H_i^∞ for the alkane/alkane binaries covering a variety of solute–solvent combinations has not been established.

Prediction methods for H_i^∞ using an equation of state (EOS) seem to have limitations in applicability arising from mixing rules. From thermodynamics, H_i^∞ is given as the product of γ_i^∞

and the fugacity of a solute i , f_i^0 ; $H_i^\infty = \gamma_i^\infty f_i^0$. Conventional prediction methods for H_i^∞ consist of the correlation of the H_i^∞ data in terms of the interaction parameters involved in the residual terms of $\ln \gamma_i^\infty$. Chappelow III and Prausnitz¹ used the UNIQUAC combinatorial entropy for the combinatorial terms of $\ln \gamma_i^\infty$ and the Flory–Huggins χ parameters for the residual terms. They correlated the H_i^∞ data for C_1 to C_4/C_{16} binaries. Rodriguez and Patterson² expressed the combinatorial term using the Flory–Huggins combinatorial entropy and a residual term with the corresponding-state principle. Neither the Flory–Huggins nor the UNIQUAC combinatorial entropy represents the experimental data for the combinatorial entropies of alkane/alkane binaries when the carbon number of solute i (N_i) is much smaller than that of the solvent j (N_j).³ To develop a universal method for predicting H_i^∞ in alkane/alkane binaries, $\ln \gamma_i^\infty$ must first be expressed with rational combinatorial and residual terms. Second, the standard-state fugacity and its composing elements that satisfactorily represent the H_i^∞ data must be specified at temperatures above the solute critical; hypothetical liquids must be adequately defined.

S. Kato's e-mail address is Kato-satoru@c.metro-u.ac.jp.

Prausnitz and Shair,⁴ Yen and McKetta Jr.⁵ reported that the relationships between the nondimensional fugacities of the saturated vapors for pure liquids at 101.3 kPa and the reduced temperature of solute i (T_{ri}) are independent of the solute types. They used the regular-solution theory to express $\ln \gamma_i^\infty$ and determined the fugacities from the solubility data of the gases. However, for the alkane/alkane binaries, the regular-solution theory fails to predict reliable values of $\ln \gamma_i^\infty$ because the theory provides a relationship, $\ln \gamma_i^\infty > 0$, in spite of the experimental proof: $\ln \gamma_i^\infty < 0$.³ The method by Rodriguez and Patterson² has limitations in its applicability because a hypothetical liquid has not been defined. Chappelow III and Prausnitz¹ defined hypothetical liquids by extending the fugacity expressions given by Prausnitz and Chueh⁶ below the solute critical to temperatures above the solute critical. This method does not lead us to a universal prediction expression because the parameters are dependent on solute type. The reason that none of the conventional studies has established a universal prediction method for H_i^∞ of the alkane/alkane binaries is ascribed to the fact that they could not use an appropriate expression for $\ln \gamma_i^\infty$.

Kato et al.³ represented $\ln \gamma_i^\infty$ data for solute alkanes in longer carbon-chain alkanes according to a first-order function of the inverse absolute temperature. The alkanes determining this expression have linear-shaped molecules; therefore, the expression should be modified for simple fluids having spherical molecules, such as methane, and providing different orientation patterns from the linear molecules around the parallel frameworks formed by the solvent molecules. In the literature, special attention has not been paid to the molecular orientations of simple fluids, and the same expressions of combinatorial entropies with those for linear molecules have been used. However, when the solute approaches a simple fluid with decreasing N_i , a modification of $\ln \gamma_i^\infty$ using the acentric factor proposed by Pitzer⁷ may be promising for the evaluation of solution structures and molecular interactions around a molecule of a simple fluid. Such a modification has not been found in the literature. As for the definition of hypothetical liquids, it seems much more definite to specify hypothetical liquids by their vapor pressures, given the great amount of knowledge on vapor pressures that has been accumulated. However, no report has been found specifying the vapor pressures and the fugacity coefficients of the saturated vapor phases of hypothetical liquids.

One of the purposes of the present study is to develop a universal prediction method for H_i^∞ of alkane/alkane binaries by the modification of $\ln \gamma_i^\infty$ given by Kato et al.³ for application to simple fluids and by the definition of hypothetical liquids in terms of vapor pressures and fugacity coefficients. The second purpose is to show that the universal prediction method practically serves to clarify solution structures in alkane/alkane binaries at infinite dilution, to verify the reliability of high-pressure vapor–liquid equilibrium (VLE) data for alkane/alkane binaries in the literature, and to predict the H_i^∞ values of rare gases in an alkane solvent.

Modeling

Modification of infinite-dilution activity coefficients for solute alkanes approaching a simple fluid

Consider a system consisting of a solution of a solute alkane i infinitely diluted in a solvent alkane j and the saturated vapor

phase contacting the solution at temperature T . The pressure dependency of Henry's law constant is given as follows⁸:

$$H_i^\infty = H_i^{\infty(Pa)} \exp[v_i^\infty(P - P_a)/RT] \quad (1)$$

where H_i^∞ and $H_i^{\infty(Pa)}$ denote Henry's law constants of the solute alkane i at a system pressure P , and at a reference pressure P_a , respectively, and v_i^∞ denotes the partial molar volume of solute i diluted in the solvent j at infinite dilution. In the present study, the unit Pa is used for representing pressures and m³ for volumes. In Eq. 1, R denotes the gas constant. Using the mole fraction of solute i in the liquid phase x_i , and the fugacity of solute i in the vapor phase f_{iV} , H_i^∞ is defined as follows

$$H_i^\infty = \lim_{x_i \rightarrow 0} (f_{iV}/x_i) \quad (2)$$

whereas $H_i^{\infty(Pa)}$ is given as follows⁸

$$H_i^{\infty(Pa)} = \gamma_i^{\infty(Pa)} \phi_{is} p_{is} \quad (3)$$

where $\gamma_i^{\infty(Pa)}$ denotes the infinite-dilution activity coefficient of solute i relative to the reference pressure P_a , and specifying the saturated liquid of solute i at T and at the saturated vapor pressure p_{is} as a standard state of activity; ϕ_{is} denotes the fugacity coefficient of the saturated vapor of solute i at temperature T . Equations 1 to 3 provide the following expression for H_i^∞

$$H_i^\infty = \gamma_i^\infty \phi_{is} p_{is} \exp\left[\frac{v_i^\infty(P - P_a)}{RT}\right] \quad (4)$$

where γ_i^∞ is identical with $\gamma_i^{\infty(Pa)}$, but, hereafter, the superscript (Pa) is abbreviated for simplicity. The value of the reference pressure P_a is fixed at 101.3 kPa throughout this study. Using a dispersion force parameter Q_{ij} , Kato et al.³ correlated the infinite-dilution activity coefficients of alkanes diluted in longer carbon-chain alkanes as follows

$$\ln(\gamma_i^\infty)_{linear} = (0.173 - 28.3/T)Q_{ij} \quad (5)$$

$$Q_{ij} = \frac{q_i - q_j}{q_i} \quad (6)$$

$$q_i = (2)(0.848) + 0.540(N_i - 2) \quad (7)$$

$$q_j = (2)(0.848) + 0.540(N_j - 2) \quad (8)$$

where q_i and q_j denote measures of the molecular surface areas of solute i and solvent j , respectively. Equation 5 represents 225 points of γ_i^∞ data for the alkanes from butane to decane, and the solvent alkanes from heptane to hexatriacontane at temperatures ranging from 280 to 373 K; therefore, a bracket $(\cdot)_{linear}$ is used to distinguish Eq. 5 for solutes having straight carbon chains from γ_i^∞ for simple fluids like methane having small spherical molecules.

In the present study, the effect of simple fluids on $\ln \gamma_i^\infty$ is

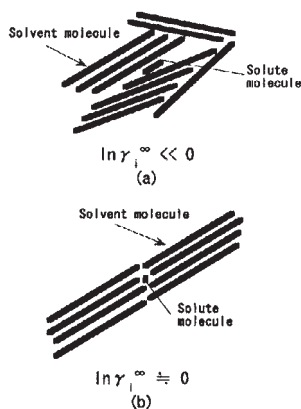


Figure 1. Destruction of the parallel frameworks: (a) by an acentric molecule, (b) by a simple-fluid molecule orientating end-to-sphere.

estimated as follows. Figure 1a schematically shows the destruction of the parallel frameworks formed in a solvent alkane by the introduction of a solute molecule having a linear chain. When the carbon chain of the solute becomes shorter, the attractive forces acting between the solute and solvent molecules become weak; therefore, the destructed frameworks of the solvent do not recover in this case. As demonstrated by Eq. 5, the decrease in $(\ln \gamma_i^\infty)_{\text{linear}} (< 0 \text{ at } 298.15 \text{ K})$ with decreasing N_i reflects this growing destruction. On the other hand, as shown by Figure 1b, when the solute approaches a simple fluid, the parallel frameworks of the solvent molecules are retained without destruction because a small spherical molecule can locate at the end of the solvent alkane's long carbon-chain molecules forming an end-to-sphere orientation; the solution approaches an ideal solution. Simple fluids are characterized by the acentric factor ω_i , proposed by Pitzer.⁷ In Figure 2, ω_i is plotted vs. q_i . The straight line drawn in Figure 2 stands for acentric factors, which are proportional to q_i , denoted as $(\omega_i)_{\text{linear}}$. The line passes through the points for nonane and decane having linear molecules. It is now expected that a difference between ω_i and $(\omega_i)_{\text{linear}}$ represents the end-to-sphere orientations shown in Figure 1b for simple fluids; the present study assumes the effect of the simple fluid on $\ln \gamma_i^\infty$ as follows

$$\ln \gamma_i^\infty = \left[\frac{\omega_i}{(\omega_i)_{\text{linear}}} \right]^m \ln(\gamma_i^\infty)_{\text{linear}} \quad (9)$$

$$(\omega_i)_{\text{linear}} = \frac{\omega_{\text{decane}}}{q_{\text{decane}}} q_i \quad (10)$$

where ω_{decane} and q_{decane} denote the acentric factor and the measure of the molecular surface area of decane, respectively. The constant m in Eq. 9 is determined from the H_i^∞ data satisfying $T < T_{ci}$, where T_{ci} denotes the critical temperature of solute i . It is stressed that γ_i^∞ in Eq. 9 is defined by the activity specifying the standard state of a pure liquid i at T and p_{is} .

Determination of p_{is} and ϕ_{is} of hypothetical liquids

It is known that the vapor pressures of hydrocarbons are well represented by the Clapeyron equation.⁹ A constant in the

equation may be a universal constant that is independent of the solute types because repulsive movements dominate the molecular interactions at $T > T_{ci}$. Therefore, in the present study, a universal Clapeyron equation is used for describing the vapor pressures of hypothetical liquids. Specifying $p_{is} = P_{ci}$ at $T = T_{ci}$, the universal Clapeyron equation and Eq. 4 provide the following equation, when $P = P_a$ holds

$$\ln \frac{H_i^\infty}{P_{ci} \gamma_i^\infty} = \ln \phi_{is} + h \left(1 - \frac{1}{T_{ri}} \right) \quad (11)$$

where h denotes the universal constant and P_{ci} is the critical pressure of solute i . If the relationships between $1 - 1/T_{ri}$ and $H_i^\infty/P_{ci} \gamma_i^\infty$ from the data covering $T > T_{ci}$ conform to a single straight line, both constants h and ϕ_{is} are determined from the linear relationship. In the following analysis, Eq. 11 is examined using the H_i^∞ data covering $T > T_{ci}$. It is one of the original ideas in the present study to determine the elements composing the fugacities of hypothetical liquids.

Data Sources and Data Selection

Data sources and characteristics of H_i^∞ data

Almost all of the H_i^∞ data of alkane solutes diluted in alkane solvents were collected from the journals pertaining to chemical engineering and chemical thermodynamics. In total, 286 data points were found from 20 references. Table 1 presents these data sources, where the solutes range from methane to decane, and the solvents from hexane to tetracosane satisfying $N_i < N_j$. The system temperatures range from 258 to 475 K. In the present study, the H_i^∞ values listed in the literature were cited without modification. These include all data from gas-liquid chromatography (GLC) and dynamic equilibrium cell (DEC) measurements. Some references from static equilibrium cells (SEC) have reported the solubilities of solutes in terms of x_i at 101.3 kPa of the solute partial pressure. In these cases, the values of γ_i^∞ from Eq. 5, assuming $\gamma_i^\infty = (\gamma_i^\infty)_{\text{linear}}$ were compared with the activity coefficients at finite compositions γ_i , predicted from the method proposed by Kato et al.²⁹ When $x_i < 0.4$, 26 points of Henry's law constants were calculated to

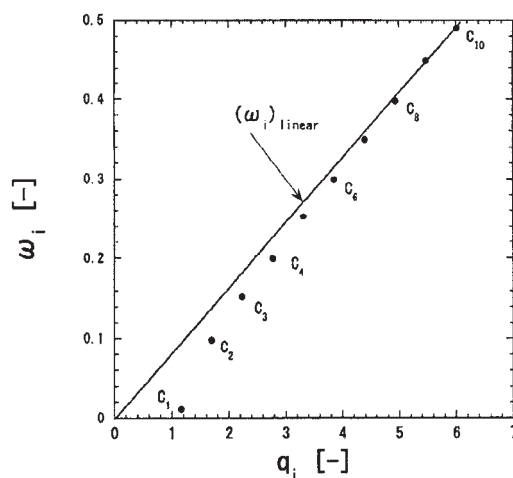


Figure 2. Relationship between q_i and ω_i .

Table 1. Data Sources for H_i^∞

Reference	Meas.*	N_{data} **	N_i/N_j^\dagger	T_{min}	T_{max}
Gjaldbaek (1952) ¹⁰	2	1	3/10	298.15	298.15
Lannung and Gjaldbaek (1960) ¹¹	1	1	1/6	298.15	298.15
Thomsen and Gjaldbaek (1963) ¹²	1	1	3/6	298.15	298.15
Ng et al. (1969) ¹³	2	50	(1,2,3)/18, (1,2,3)/20, (1,2,3)/22	308.15	473.15
Lenoir et al. (1971) ¹⁴	2	7	(1,2,3,4)/16, (2,3,4)/17	298.15	323.15
Jadot (1972) ¹⁵	2	11	2/10, 3/(6,7,8,9,10), 4/(6,7,8,9,10)	298.15	298.15
Hayduk et al. (1972) ¹⁶	1	10	3/(6,7,12,16)	298.15	318.1
Hayduk and Castaneda (1973) ¹⁷	1	10	3/(6,16,17), 4/(6,7,8,12,16,17)	298.15	323.15
Chappelow, III and Prausnitz (1974) ¹	1	44	(3,4)/16, (1,2,3,4)/20	300	475
Fleury and Hayduk (1975) ¹⁸	1	4	3/6	258.1	323.15
King and Al-Najjar (1977) ¹⁹	1	7	3/(12,14,16)	303.1	343.1
Richon and Renon (1980) ²⁰	3	8	(1,2,3,4)/16, (1,2,3,4)/18	298.15	323.15
Parcher and Johnson (1980) ²¹	2	20	(1,2,3,4,5)/16	298.15	328.15
Monfort and Arriaga (1980) ²²	2	12	(2,3,4)/10, (2,4)/12	278.1	323.15
De Ligny and van Houwelingen (1986) ²³	1	1	1/10	298.15	298.15
Gonzalez et al. (1987) ²⁴	1	22	3/(8,9,10,12,13,14,15), 4/(8,9,10,12,13,14,15)	298.15	323.15
Hayduk et al. (1988) ²⁵	1	5	(3,4)/8	298.15	343.15
Colson and Vanhove (1990) ²⁶	3	43	(5,8)/16, (2,4,5,6,7,8,10)/20	333	473
Zuliani et al. (1993) ²⁷	2	18	(3,4,5)/16, (3,4,5)/24	303.15	373.15
Hesse et al. (1996) ²⁸	1	11	1/(6,7,8,9,10,11,12,13,14,15,16)	298.15	298.15

* Measuring method: 1, static equilibrium cell; 2, gas-liquid chromatography; 3, dynamic equilibrium cell.

**Number of data.

†Carbon numbers, N_i for solute and N_j for solvent, are bracketed if the same solvent or solute is used.

be $1.013 \times 10^5/x_i$ because $0.98 < \gamma_i/\gamma_i^\infty < 1.02$ is satisfied. Table 1 includes the references of these 26 points.

In Figure 3, $\ln H_i^\infty$ is plotted vs. $1/T$ for the solvents hexadecane. In Figure 3, the $\ln H_i^\infty$ values calculated from the empirical correlation by Harvey³⁰ are shown by the dotted lines. Harvey's correlation is well represented by straight lines; therefore, a straight line representing pentane is drawn in Figure 3. In Figure 4, the $\ln H_i^\infty$ data at 298.15 K for the solvent hexadecane are plotted vs. N_i .

The relationships between $\ln H_i^\infty$ and N_j are almost linear; therefore, experimental errors are estimated by the average absolute deviations (AADs) of the $\ln H_i^\infty$ data from the corre-

lation, $\ln H_{i,cal}^\infty = a + bN_j$. The values of $(AAD)_{\ln H}$, defined as $(AAD)_{\ln H} = (100/N_{data}) \sum |(\ln H_{i,exp}^\infty - \ln H_{i,cal}^\infty)/\ln H_{i,exp}^\infty|$, were calculated for 66 data points at 298.15 K, where N_{data} denotes the number of results. The value of $(AAD)_{\ln H}$ is as small as 0.28%, where that of 37 points from SEC is 0.19% and is <0.33% for 23 points from GLC. The average value of $(AAD)_{\ln H}$ from GLC and SEC is 0.24% $[(0.33 \times 23 + 0.19 \times 37)/60]$; therefore, DEC provides an intermediate value of $(AAD)_{\ln H}$ between those from SEC and GLC. If the experimental errors are estimated by $(AAD)_H$ between $H_{i,exp}^\infty$ and $H_{i,cal}^\infty$, defined as $(AAD)_H = (100/N_{data}) \sum |(H_{i,exp}^\infty - H_{i,cal}^\infty)/H_{i,exp}^\infty|$, the average $(AAD)_H$ for 66 points is 4.0%, whereas that from SEC is as low as 2.7%.

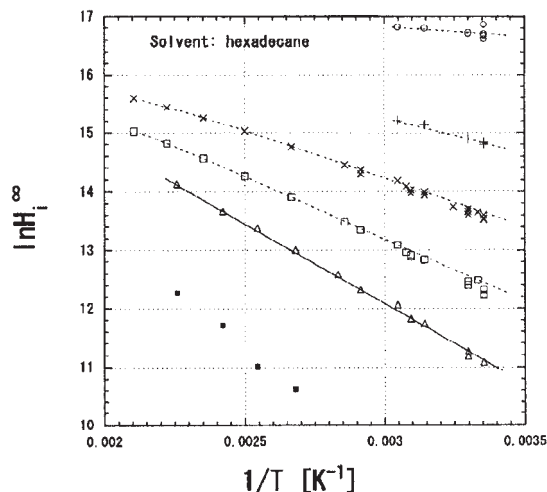


Figure 3. Relationships between reciprocal absolute temperature and $\ln H_i^\infty$ with a solvent hexadecane.

(○) methane; (+) ethane; (×) propane; (□) butane; (△) pentane; (■) octane; (---) correlation by Harvey³⁰ for C_1 to C_4 ; (—) linear regression.

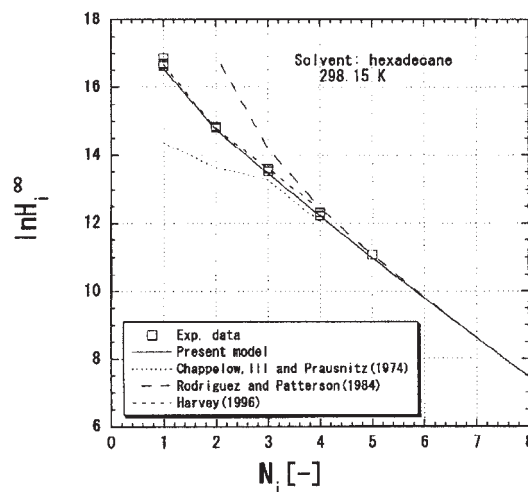


Figure 4. Relationships between N_i and $\ln H_i^\infty$ with a solvent hexadecane at 298.15 K.

Data selection for analysis

The relationship between $\ln H_i^\infty$ and $1/T$ typically conforms to a single line for the same solute–solvent combination. However, single lines cannot be found for a few data sets. When $(AAD)_{\ln H} > 0.004$, a single relationship between $1/T$ and $\ln H_i^\infty$ is hardly determined because of the large data fluctuations. Therefore, in the following analysis, all the data points involved in the data sets ranging from $(AAD)_{\ln H} > 0.004$ are eliminated to ensure a definite quantitative analysis. Of the data in Table 1, 46 points were eliminated based on this limitation. The other 240 points are used in the analysis. Of the 46 points eliminated from the analysis, 29 points were measured using eicosane as the solvent. Morgan and Kobayashi³¹ applied zone refining to eicosane and recognized two refined zones, that is, the top cut and the middle cut, having almost identical freezing points and boiling points; therefore, the data fluctuation in H_i^∞ with the solvent eicosane may arise from the impurity involved in eicosane.

Determination of Model Parameters

Physical properties

Vapor pressures were calculated by the Wagner equation, the Antoine equation, or the Frost–Kalkwarf–Thodos equation with the parameters recommended by Reid et al.⁹ The King and Al-Najjar equation³² is also used for the C₉, C₁₀, C₁₂, C₁₄, and C₁₆ alkanes. The vapor pressures were set equal to zero for high-boiling alkanes where neither the Wagner equation nor the King–Al-Najjar equation can be used. Compared with the experimental vapor pressures for C₂ to C₈ and C₁₆ alkanes, the values of AAD in p_{is} do not exceed 0.84% except for hexadecane for which the vapor–pressure data fluctuate within 6%. Acentric factors recommended by Reid et al.⁹ were used.

The fugacity coefficient of the saturated vapor for the alkane i , ϕ_{is} , is calculated as follows

$$\ln \phi_{is} = \int_0^{p_{is}} \frac{Z_i - 1}{P} dP \quad (12)$$

where Z_i denotes the compressibility factor of the saturated vapor of solute i . The values of the critical compressibility factors (Z_{ic}) for methane to butane calculated from the Benedict–Webb–Rubin (BWR) EOS were 0.288 to 0.274, respectively, and these are identical with the experimental values.⁹ Meanwhile, the fugacity coefficient at the critical points ϕ_{ic} , calculated from the BWR EOS, was independent of the type of alkanes from methane to butane, that is, 0.655. The Soave–Redlich–Kwong (SRK) and Peng–Robinson (PR) EOSs determined ϕ_{ic} to be 0.666 and 0.643, respectively. In the present study, the BWR EOS is used for the calculation of ϕ_{is} for methane to butane, whereas the SRK EOS is used for pentane and heavy alkanes for simplicity. The error from SRK EOS does not affect the results because the error is 1.7%, which is much less than the experimental error.

To estimate the magnitude of the experimental errors in γ_i^∞ , 36 points of γ_i^∞ data at 353 K were chosen from Table 1 in the reference by Kato et al.³ The value of $(AAD)_\gamma$, defined as $(AAD)_\gamma = (100/N_{data}) \sum |(\gamma_{i,exp}^\infty - \gamma_{i,cal}^\infty)/\gamma_{i,exp}^\infty|$ using the first-order regression, $\ln \gamma_{i,cal}^\infty = a + bN_j$, was calculated for

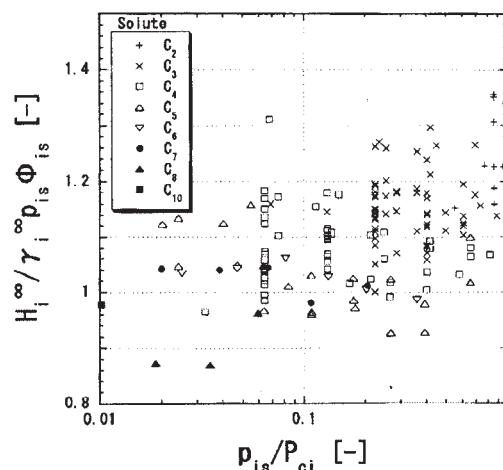


Figure 5. Relationships between p_{is}/P_{ci} and $H_i^\infty/\gamma_i^\infty p_{is}\phi_{is}$ calculated with $m = 0$.

the 36 points, and the value of $(AAD)_\gamma$ is 1.6%. Therefore, $(\gamma_i^\infty)_{linear}$ in Eq. 5 can represent the γ_i^∞ data within a 1.6% AAD. On the other hand, Lyckman et al.³³ showed that an alkane/alkane system can be treated as a nonexpanded solvent when the nondimensional parameter, $TP_{ci}/(\Delta H_f/v_{js})T_{ci}$, is < 0.06 . The $TP_{ci}/(\Delta H_f/v_{js})T_{ci}$ values calculated for all the data in Table 1 are < 0.06 except for only one case, that is, 0.063 for methane/docosane at 473.15 K. Therefore, in the present analysis, v_i^∞ was approximated to be equal to the molar volume of the saturated liquid i , v_{is} .

The value of m

The constant m is determined using the H_i^∞ data covering temperatures below the solute critical. The values of the exponential term in Eq. 4 ranged from $0.988 < \exp[v_{is}(P - 101.3)/RT] < 1.012$; therefore, in the present study, the exponential term in Eq. 4 is neglected. To examine the effect of $[\omega/(\omega_i)_{linear}]^m$ on H_i^∞ , in Figure 5, the $H_i^\infty/\gamma_i^\infty p_{is}\phi_{is}$ data covering $T < T_{ci}$ is plotted vs. p_{is}/P_{ci} , where m was fixed at zero. It is apparent from Figure 5 that $H_i^\infty/\gamma_i^\infty p_{is}\phi_{is}$ deviates from unity when the carbon number decreases. The average absolute deviation $(AAD)_1$, defined by the following equation

$$(AAD)_1 = (100/N_{data}) \sum |(H_i^\infty/\gamma_i^\infty p_{is}\phi_{is})_{exp} - 1| \quad (13)$$

is 11.3% for 169 points of the H_i^∞ data covering $T < T_{ci}$. The value of $(AAD)_1$ is obviously greater than the sum of AAD of the H_i^∞ measurement and the prediction of γ_i^∞ , p_{is} , and ϕ_{is} , that is, 7.1% ($= 4 + 1.6 + 0.8 + 1.7$). Accordingly, the failure of the accurate prediction of H_i^∞ at $T < T_{ci}$ arises from not using the $[\omega/(\omega_i)_{linear}]^m$ term.

In the next step, to determine the value of m from the thermodynamic relationship, that is, Eq. 4, the values of $(AAD)_1$ were calculated with the 169 points of the H_i^∞ data satisfying $T < T_{ci}$. The values of $(AAD)_1$ for $m = 0, 1, 2, 3$, and 4 are 11.3, 8.6, 6.8, 5.9, and 5.6%, respectively. When $m = 3$, $(AAD)_1$ is well below 7.1%, and $H_i^\infty/\gamma_i^\infty p_{is}\phi_{is}$ tends to be equal to unity vs. the variation in p_{is}/P_{ci} . However, when a value of 4 or higher is chosen for m , $H_i^\infty/\gamma_i^\infty p_{is}\phi_{is}$ decreases with in-

Table 2. AADs between Experimental and Predicted H_i^∞ Values for 240 Points of Data

	$(AAD)_H^a(N_{data})$									
	C ₁	C ₂	C ₃	C ₄	C ₅	C ₆	C ₇	C ₈	C ₁₀	Average
$T < T_{ci}$		5.0 (11)	6.3 (65)	5.2 (57)	6.1 (21)	2.1 (6)	2.4 (5)	11.9 (3)	1.8 (1)	5.7 (169)
$T > T_{ci}$	13.7 (25)	5.5 (18)	4.1 (21)	2.1 (6)	0.2 (1)					7.6 (71)
Total	13.7 (25)	5.3 (29)	5.8 (86)	4.9 (63)	5.8 (22)	2.1 (6)	2.4 (5)	11.9 (3)	1.8 (1)	6.2 (240)

$$^a(AAD)_H = (100/N_{data}) \sum |(H_{i,exp}^\infty - H_{i,cal}^\infty)/H_{i,exp}^\infty|$$

creasing p_{is}/P_{ci} . Accordingly, in the present study, m is fixed at 3, and $\ln \gamma_i^\infty$ is given as follows for representing the H_i^∞ data at $T < T_{ci}$

$$\ln \gamma_i^\infty = \left[\frac{\omega_i}{(\omega_i)_{linear}} \right]^3 \ln(\gamma_i^\infty)_{linear} \quad (14)$$

If Eq. 14 is used, the $H_i^\infty/\gamma_i^\infty p_{is}\phi_{is}$ data distribute near unity for any value of p_{is}/P_{ci} covering $p_{is}/P_{ci} < 1$. In Table 2, the values of $(AAD)_H$ are listed for each alkane solute as calculated with Eq. 14 using the 169 H_i^∞ data points satisfying $T < T_{ci}$. The $(AAD)_H$ for octane is large, because the three data points for H_i^∞ involve relatively large data fluctuations.

The value of the universal constant h

To examine the applicability of Eq. 11, in Figure 6, the $H_i^\infty/P_{ci}\gamma_i^\infty$ data at $T > T_{ci}$ are plotted vs. $1 - 1/T_{ri}$. The values of γ_i^∞ were calculated from Eq. 14. For methane $\omega_i = 0.008$ proposed by Yokoyama et al.³⁴ was used because the data convergence in Figure 6 for methane is better than the case where $\omega_i = 0.011$ calculated from the Wagner equation⁹ is used. The value of q_i for methane is also calculated from Eq. 7 without modification. The value of ϕ_{iC} from the BWR EOS is equal to 0.655 and is marked in Figure 6. Figure 6 shows that the linear trend in the data is independent of the types of alkane/alkane binaries. Furthermore, the $H_i^\infty/P_{ci}\gamma_i^\infty$ data tend to intersect at the intercept of 0.655, demonstrating that Eq. 14 is rational for representing the H_i^∞ data and that the following equation holds for hypothetical liquids

$$\phi_{is} = \phi_{iC} \quad (T > T_{ci}) \quad (15)$$

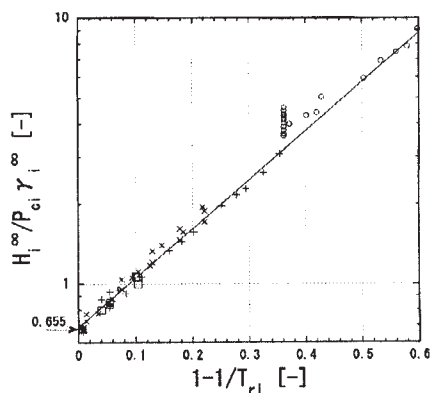


Figure 6. Relationships between $1 - 1/T_{ri}$ and $H_i^\infty/P_{ci}\gamma_i^\infty$ with the data satisfying $T > T_{ci}$.

(○) methane; (+) ethane; (×) propane; (□) butane; (—) Eq. 16.

To determine a reliable value of h , first, an average value of h (h_{ave}) was determined from the data regression according to Eq. 11, and those data covering $AAD > 5\%$ were eliminated. The remaining data provide an average, $h_{ave} = 4.5$; therefore, the expression of the vapor pressures for hypothetical liquids is established as follows

$$\ln \frac{p_{is}}{P_{ci}} = 4.5 \left(1 - \frac{1}{T_{ri}} \right) \quad (T > T_{ci}) \quad (16)$$

The solid line in Figure 6 stands for Eq. 16. Table 2 includes the values of $(AAD)_H$ for the data covering $T > T_{ci}$. Combining Eq. 15 and the definition of the acentric factor proposed by Pitzer,⁷ the value of the acentric factor for the hypothetical liquids ω_h , is given as

$$\omega_h = -0.16 \quad (17)$$

It has been demonstrated that when $T_{ri} > 3$, the relationships between the $\ln H_i^\infty$ data and $1/T_{ri}$ do not conform to a straight line.^{4,30} As shown in Figure 6, all the data used in the present study conform to a straight line because they cover the range $1 < T_{ri} < 3$; therefore, it should be stressed that Eqs. 15 to 17 hold only when $1 < T_{ri} < 3$.

In the literature, hypothetical liquids have been identified by the fugacity values. In the present study, not only p_{is} and ϕ_{is} , but also the heats of vaporization (ΔH_v) and the molar volumes of hypothetical liquids (v_L^0) are estimated from the thermodynamic results. They are summarized as follows: (1) p_{is} is given by Eq. 16, whereas (2) $\phi_{is} = \phi_{iC}$ and $Z_v = 1$; (3) $\Delta H_v = 0$; and (4) $v_L^0 = RT/p_{is}$ hold. It follows from Eqs. 12 and 15 that the compressibility factor of the saturated vapor phase for a hypothetical liquid is equal to unity; therefore, neither the vapor phase nor liquid phase includes molecular interactions. This results in $\Delta H_v = 0$. From thermodynamics, $h = \Delta H_v/R(Z_v - Z_L)$ holds, whereas $\Delta H_v = 0$ and $h > 0$ hold from the above analysis. Therefore, Z_L is identical to Z_v , which is equal to unity. The hypothetical liquids then have molar volumes given as RT/p_{is} . In the following analysis, RT/p_{is} is used if the values of v_L^0 for hypothetical liquids are needed.

Prediction of H_i^∞

Using Eq. 18, the H_i^∞ data for the solute alkane i and the solvent alkane j are transformed into the H_i^∞ data for the solute alkane i and a hexadecane solvent, where Eqs. 4 and 14 are used for the derivation of the following equation

$$H_{i,HD}^\infty = H_i^\infty \exp \left\{ \left[\frac{\omega_i}{(\omega_i)_{linear}} \right]^3 \left(0.173 - \frac{28.3}{T} \right) (Q_{i,HD} - Q_{ij}) \right\} \quad (18)$$

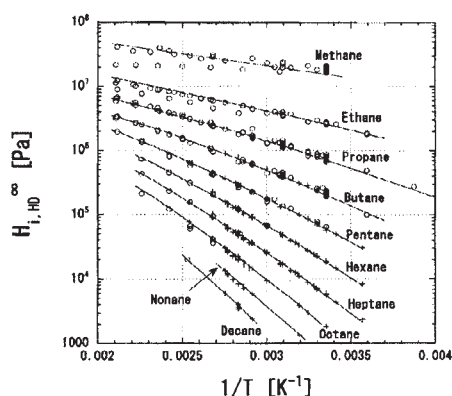


Figure 7. Comparison between experimental and predicted Henry's law constants for a solvent hexadecane.

(○) 286 points from Henry's law constant data; (+) 225 points from infinite-dilution activity coefficient data; (—) predicted from the model proposed in the present study (Eqs. 4 and 14–16).

In Figure 7, Henry's law constants with the solvent hexadecane, $H_{i,HD}^{\infty}$, are plotted vs. $1/T$ using the key ○ for all of the 286 data points. Also, the transformed values of $(\gamma_i^{\infty})_{linear}$ for the solvent hexadecane were calculated to express $H_{i,HD}^{\infty}$ as follows

$$H_{i,HD}^{\infty} = p_{is} \phi_{is} (\gamma_i^{\infty})_{linear} \exp \left\{ \left[\frac{\omega_i}{(\omega_i)_{linear}} \right]^3 \times \left(0.173 - \frac{28.3}{T} \right) (Q_{i,HD} - Q_{ij}) \right\} \quad (19)$$

The data from the 225 points for $(\gamma_i^{\infty})_{linear}$ compiled by Kato et al.³ were used. In Figure 7, $H_{i,HD}^{\infty}$ calculated from Eq. 19 is plotted using the key +. In Figure 7, the solid lines stand for $H_{i,HD}^{\infty}$ predicted from Eqs. 4 and 14–16. The data convergence for methane, ethane, and octane is worse. In Figure 7, the $H_{i,HD}^{\infty}$ values represented by the symbols ○ and + are in excellent agreement with those represented by the solid lines; the present universal prediction method can accurately predict Henry's law constants of the alkane/alkane binaries. The present model has been found to fit 84% of the 286 experimental values for $H_{i,HD}^{\infty}$ to within $\pm 6.2\%$ AAD.

In Figure 4, the relationships between N_i and the predicted values of $\ln H_{i,HD}^{\infty}$ for alkanes in hexadecane at 298.15 K are shown. Harvey³⁰ correlated the $H_{i,HD}^{\infty}$ data with temperature for only the C_1 to C_4/C_{16} binaries. Chappelow III and Prausnitz¹ defined hypothetical liquids, but they introduced seven parameters for a solute–solvent combination for the limited systems consisting of the C_1 to C_4/C_{16} binaries. Rodriguez and Patterson² represented the residual terms of $\ln \gamma_i^{\infty}$ with five universal parameters. However, they did not define a hypothetical liquid. The latter two methods predict much different values of $H_{i,HD}^{\infty}$ from the experimental values for the light alkanes. Therefore, the application of the conventional three methods are considerably limited, and no reliable universal prediction method for $H_{i,HD}^{\infty}$ is found in the literature. On the other hand, the method proposed in the present study satisfactorily predicts the values of $H_{i,HD}^{\infty}$ for a variety of solute–solvent combinations covering the

C_1 to C_{10}/C_6 to C_{24} binaries in spite of the limited parameters, m and h . The modifications of $H_{i,HD}^{\infty}$ by these two parameters are obviously original ideas proposed for the first time in the present study.

Application of the Present Model

Solution structures of simple fluid/alkane binaries at infinite dilution

It is now possible to discuss the relationships between the solution structures and the standard states of activities using the established prediction method for $\ln \gamma_i^{\infty}$ (Eq. 14). An infinite-dilution activity coefficient defined by the standard-state fugacity of solute i at T and p_{is} , γ_i^{∞} , and that at T and P_a , $\gamma_{i(Pa)}^{\infty}$, are different by the magnitude of Poynting factor defined as follows⁸

$$\gamma_i^{\infty} = \gamma_{i(Pa)}^{\infty} \exp \frac{v_i^0 (P_a - p_{is})}{RT} \quad (20)$$

where a reference pressure P_a , for both γ_i^{∞} and $\gamma_{i(Pa)}^{\infty}$ is fixed at 101.3 kPa, and the superscript (P_a) has been abbreviated from $\gamma_{i(Pa)}^{\infty}$ and $\gamma_{i(Pa)}^{\infty}$. In Figure 8, the values of $\ln \gamma_{i(Pa)}^{\infty}$ and $\ln \gamma_i^{\infty}$ for alkane solutes from methane to decane in hexadecane at 298.15 K are plotted vs. N_i , where γ_i^{∞} was calculated from Eq. 14, and the molar volume of the liquid (v_i^0) was determined by the Rackett equation.⁹ When $T > T_{ci}$, $v_i^0 = RT/p_{is}$ was used. Figure 8 shows that $\gamma_i^{\infty} = \gamma_{i(Pa)}^{\infty}$ holds, when the vapor pressures of the solutes are low. However, when the solute approaches a simple fluid, $\ln \gamma_{i(Pa)}^{\infty} \gg 0$ holds because of the decreases in the values of the Poynting factor, whereas $\ln \gamma_i^{\infty}$ approaches zero, showing the rational trend that the solutions approach an ideal solution. To clarify the irrational trend of $\ln \gamma_{i(Pa)}^{\infty}$, the partial molar excess enthalpy of solute i , $h_{i(Pa)}^{E,\infty}$ was calculated from $\partial \ln \gamma_{i(Pa)}^{\infty} / \partial (1/T) = h_{i(Pa)}^{E,\infty} / R$ and the entropy, $s_{i(Pa)}^{E,\infty}$, from $-s_{i(Pa)}^{E,\infty} / R = \ln \gamma_{i(Pa)}^{\infty} - h_{i(Pa)}^{E,\infty} / RT$. Figure 8 includes the calculated values of $-s_{i(Pa)}^{E,\infty} / R$ and $h_{i(Pa)}^{E,\infty} / RT$. Figure 8 shows that absurd relationships $s_{i(Pa)}^{E,\infty} < 0$ and $h_{i(Pa)}^{E,\infty} < 0$ hold

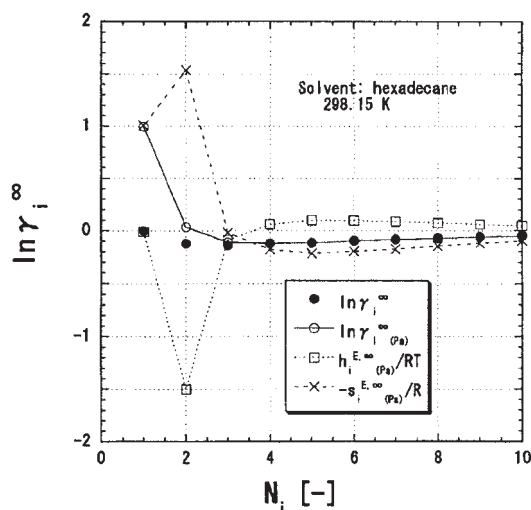


Figure 8. Relationships between N_i and $\ln \gamma_i^{\infty}$ for a solvent hexadecane at 298.15 K.

$h_{i(Pa)}^{E,\infty}$ and $s_{i(Pa)}^{E,\infty}$ were calculated from $\ln \gamma_{i(Pa)}^{\infty}$.

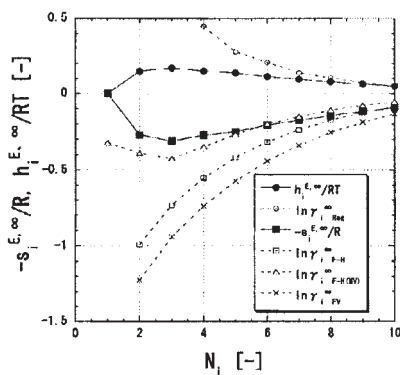


Figure 9. Relationships between N_i and $h_i^{E,\infty}/RT$ and $-s_i^{E,\infty}/R$ for a solvent hexadecane at 298.15 K. $h_i^{E,\infty}$ and $s_i^{E,\infty}$ were calculated from $\ln \gamma_i^{\infty}$.

for light alkanes. The absurdity arises from the increase in $\ln \gamma_{i(Pa)}$ caused by the decrease in the Poynting factor; therefore, $\ln \gamma_i^{\infty}$ is convenient for describing the solution structures around a solute molecule, when the Poynting factor is remote from unity. Such a discussion is not possible until the accurate prediction method for H_i^{∞} of simple fluids is established.

$\ln \gamma_i^{\infty}$ predicted from conventional models

In Figure 9, the values of $h_i^{E,\infty}/RT$ (●) derived from the inverse temperature derivative of $\ln \gamma_i^{\infty}$ and the corresponding $-s_i^{E,\infty}/R$ values (■) are plotted vs. N_i for a hexadecane solvent at 298.15 K; they were calculated as $\partial \ln \gamma_i^{\infty} / \partial (1/T) = h_i^{E,\infty}/R$ and $-s_i^{E,\infty}/R = \ln \gamma_i^{\infty} - h_i^{E,\infty}/RT$. Figure 9 shows a relationship, $s_i^{E,\infty} > 0$, reflecting the destruction of the parallel frameworks formed in solvent alkanes by the introduction of a solute molecule. It also shows that, for a molecule of a simple fluid, the parallel frameworks are retained without destruction because $s_i^{E,\infty}$ is almost equal to zero for methane. An entropy–enthalpy compensation, $-298.15 s_i^{E,\infty} / h_i^{E,\infty} = -1.8$, holds for any solute–solvent combination at infinite dilution and at 298.15 K.

Infinite-dilution activity coefficients defined by the regular-solution theory, $\ln \gamma_{i Reg}^{\infty}$, are given as follows⁹

$$\ln \gamma_{i Reg}^{\infty} = v_i^0 (\delta_i - \delta_j)^2 / RT \quad (21)$$

$$\delta_i = [(\Delta H_{Vi} - RT) / v_i^0]^{0.5} \quad (22)$$

Figure 9 includes $\ln \gamma_{i Reg}^{\infty}$ values for the solutes from butane to decane in a hexadecane solvent at 298.15 K. Figure 9 shows that the values of $\ln \gamma_{i Reg}^{\infty}$ noticeably increase with decreasing N_i . It reaches five at ethane, demonstrating that it runs the risk of using the regular-solution theory for those alkane/alkane binaries when $Q_{ij} \ll 0$. Figure 9 also includes the Flory–Huggins combinatorial entropy, $\ln \gamma_{i F-H}^{\infty}$ and $\ln \gamma_{i F-H(MV)}^{\infty}$, defined as follows

$$\ln \gamma_{i F-H}^{\infty} = \ln \frac{q_i}{q_j} + 1 - \frac{q_i}{q_j} \quad (23)$$

$$\ln \gamma_{i F-H(MV)}^{\infty} = \ln \frac{v_i^0}{v_j^0} + 1 - \frac{v_i^0}{v_j^0} \quad (24)$$

The Flory–Huggins equation is commonly expressed by a ratio of the measures of molecular volumes.⁹ However, as shown by Eq. 23, it is replaced using molecular surface areas because dispersion forces dominate the attractive molecular interactions in the alkane/alkane binaries. Equation 24 modifies the ratio using molar volumes. The UNIQUAC combinatorial entropy⁹ is not shown in Figure 9, but it is almost equivalent to $\ln \gamma_{i F-H}^{\infty}$ when $N_i \ll N_j$. Figure 9 also includes the free-volume combinatorial entropy, $\ln \gamma_{i FV}^{\infty}$, defined as follows³⁵

$$\ln \gamma_{i FV}^{\infty} = \ln \frac{v_i^0 - v_i^*}{v_j^0 - v_j^*} + 1 - \frac{v_i^0 - v_i^*}{v_j^0 - v_j^*} \quad (25)$$

where v_i^* and v_j^* denote the van der Waals volumes of solute i and j , respectively; they were calculated from the SRK EOS. The values of $\ln \gamma_{i F-H}^{\infty}$ and the modified quantities are expected to represent the values of $-s_i^{E,\infty}/R$ for athermal solutions. Figure 9 demonstrates that $\ln \gamma_{i F-H(MV)}^{\infty}$ is most close to $-s_i^{E,\infty}/R$. However, these quantities are different from each other because $\ln \gamma_{i F-H(MV)}^{\infty}$ is substantially temperature dependent, and $-s_i^{E,\infty}/R$ is temperature independent. Figure 9 shows that both $\ln \gamma_{i F-H}^{\infty}$ and $\ln \gamma_{i FV}^{\infty}$ noticeably deviate from $-s_i^{E,\infty}/R$ when N_i decreases. Consequently, it has been demonstrated that conventional prediction methods provide large deviations from $-s_i^{E,\infty}/R$ and $h_i^{E,\infty}/RT$, when the solute approaches a simple fluid.

Identification of reliable high-pressure VLE data

Using Eqs. 4 and 14–16, the reliability of high-pressure VLE data for alkane/alkane binaries can be evaluated. The measured values of P , T , x_i , and the solute mole fraction in the vapor phase y_i are inferred to be reliable, if $\phi_j^0 y_i P / x_i$ approaches the value of H_i^{∞} predicted by the present method when the solution approaches an infinite-dilution condition; ϕ_j^0 denotes the vapor-phase fugacity coefficient of the solvent at T and p_{js} . The high-pressure VLE data compiled in the DECHEMA chemistry data series³⁶ and recent data^{37–39} for alkane/alkane binaries were examined. The examinations were limited to those data satisfying $0 < x_i < 0.1$. In total, 42 sets of data from different references for different solute–solvent combinations were obtained. If the values of $\phi_j^0 y_i P / x_i H_i^{\infty}$ are plotted vs. θ_i , which is identical with $q_i x_i / (q_i x_i + q_j x_j)$, the data significantly fluctuate, exceeding 20% from the average values of $\phi_j^0 y_i P / x_i H_i^{\infty}$. Therefore, in the present study, the infinite-dilution conditions were determined as follows: The activity coefficients for alkane/alkane binaries are well described by the Wohl equation²⁹

$$\ln \gamma_i = (1 - \theta_i)^2 \left[A + 2 \left(B \frac{q_i}{q_j} - A \right) \theta_i \right] \quad (26)$$

where $A = \ln \gamma_i^{\infty}$ and $B = \ln \gamma_j^{\infty}$ hold. For alkane/alkane binaries, the relationship $A = B$ roughly holds²⁹; therefore, assuming that an infinite-dilution condition is attained when $\ln \gamma_i$ approaches 80% of $\ln \gamma_i^{\infty}$, x_i satisfying the equation, $0.8 = (1 - \theta_i)^2 [1 + 2(q_i/q_j - 1)\theta_i]$, was determined. Denoting this x_i

Table 3. High-Pressure VLE Data Providing Converged $\phi_j^0 \gamma_j P/x_j H_{i,cal}^\infty$ Values under Dilute Conditions

N_i	N_j	$Y_{i,ave}^*$	$(AAD)_1^{**}$	N_{data}^\dagger	Reference	T_{ri}
3	10	0.86	14	8	Reamer and Sage (1966) ³⁶	1.20–1.38
3	5	0.81	19	11	Sage and Lacey (1940) ³⁶	0.93–1.25
3	4	0.85	15	3	Beranek and Wichterle (1981) ³⁸	0.87–0.98
2	10	0.89	15	8	Reamer and Sage (1962) ³⁶	1.24–1.67
2	4	0.82	18	2	Lhotak and Wichterle (1981) ³⁷	0.99
2	3	1.08	9	14	Blanc and Setier (1988) ³⁹	0.64–0.88
1	6	0.94	17	16	Gunn et al. (1976) ³⁶	1.63–2.16
1	5	1.05	15	145	Berry and Sage (1970) ³⁶	1.46–1.90
1	2	1.16	16	16	Wichterle and Kobayashi ³⁶	0.90–1.12

* $Y_{i,ave} = [\phi_j^0 y_i P/x_i H_{i,cal}^\infty]_{ave}$.

** $(AAD)_1 = (100/N_{data}) \sum |[(\phi_j^0 y_i P/x_i)_{exp}/H_{i,cal}^\infty - 1]|$.

† Number of data satisfying $x_i < x_{i,lim}$.

as $x_{i,lim}$, these data satisfying $x_i < x_{i,lim}$ were used for the determination of the average values of $\phi_j^0 y_i P/x_i H_i^\infty$, $[\phi_j^0 y_i P/x_i H_i^\infty]_{ave}$, and AAD from unity, $(AAD)_1$. Of the 42 sets of VLE data examined, nine sets satisfy the reliability criteria, that is, $0.8 < [\phi_j^0 y_i P/x_i H_i^\infty]_{ave} < 1.2$ and $(AAD)_1 < 20\%$. These nine sets are listed in Table 3. Accordingly, the present study identifies these nine data sets as the most reliable high-pressure VLE data for alkane/alkane binaries. The primary significance of this consequence is that the identified data effectively promote the development of a reliable model for describing the high-pressure VLE. The secondary significance is that the present model can satisfactorily be applied to light alkane/light alkane binaries including the ethane and propane solvents.

Infinite-dilution activity coefficients of rare gases in an alkane

It is possible to define γ_i^∞ for rare gases in alkanes if the definition of hypothetical liquids established in the present study is extended to the H_i^∞ data of rare gases. Because Pitzer⁷ classified Ar, Kr, Xe, and CH₄ into simple fluids, the γ_i^∞ values for these gases were determined from Eq. 4 with the data of H_i^∞ in hexadecane at 298.15 K. To compare the γ_i^∞ values with those for alkanes, the q_i values for rare gases are determined from the following correlation, given that the equation can be established with the C₁ to C₁₀ alkanes

$$q_i = -0.73731 + 1894S_i \quad (27)$$

where S_i is a measure of the molecular surface area defined by the van der Waals volume v_i^* , as follows: $S_i = (v_i^*)^{2/3}$. The values of q_i for rare gases were calculated from Eq. 27, and the values of γ_i^∞ , which are equivalent to the alkanes, $(\gamma_i^\infty)_{alkane}$, were calculated from Eq. 14. Table 4 includes the $\gamma_i^\infty/(\gamma_i^\infty)_{alkane}$ values for the rare gases. Allowing for a 10% error, Table 4 shows that the present method can satisfactorily predict Henry's law constants of rare gases in hexadecane. The molecular surface areas of these gases are almost equivalent to that of methane because $0.8 < S_i/S_{methane} < 1.1$ holds, whereas the ratio ω_i/S_i is smaller than that of methane: $(\omega_i/S_i)/(\omega_i/S_i)_{methane} < 1$. A similar analysis was applied to nonpolar substances, such as CCl₄ and CF₄ having spherical molecules and O₂, N₂, and CO₂ having large acentric factor values. As shown in Table 4, CCl₄ has the same values of $S_i/S_{methane}$ and $(\omega_i/S_i)/(\omega_i/S_i)_{methane}$ with those of pentane; therefore, $\gamma_i^\infty = (\gamma_i^\infty)_{alkane}$ holds, and the present prediction method for H_i^∞ can satisfactorily be used for CCl₄. However, CF₄, which has the same $S_i/S_{methane}$ value as that of ethane, shows a considerable acentricity because $(\omega_i/S_i)/(\omega_i/S_i)_{methane}$ is much larger than that of ethane. Therefore, $\gamma_i^\infty \gg (\gamma_i^\infty)_{alkane}$ holds. Accordingly, if a substance has the same acentric factor value with the alkane that has the same molecular surface area with the substance, the prediction method for H_i^∞ proposed in the present study can be applied with high accuracy. However, modifications are required for those substances showing a strong acentricity, such as O₂, N₂, CF₄, and CO₂.

Table 4. Values of γ_i^∞ Calculated from the H_i^∞ Data for Nonpolar Gases and Liquids in Hexadecane at 298.15 K

Solute	$H_i^\infty \times 10^5$ (Pa)*	$S_i/S_{methane}$	ω_i	$(\omega_i/\omega_{methane})/S_i/S_{methane}$	$\gamma_i^\infty/(\gamma_i^\infty)_{alkane}$	298.15/ T_{ci}
Simple fluids						
Ar	354 ^a	0.81	0.001	0.15	1.18	1.98
Kr	121 ^a , 151 ^b	0.93	0.005	0.67	0.86, 1.08	1.42
Xe	38.9 ^b	1.11	0.008	0.90	0.88	1.03
CH ₄	166 ^a	1	0.008	1	1.09	1.57
Spherical						
CCl ₄	0.14 ^b	2.03	0.193	11.91	1.00	0.54
Nonspherical						
Ethane	27.6 ^c	1.3	0.099	9.53	1.09	0.98
Pentane	1.41 ^b	2.17	0.197	11.33	0.92	0.69
O ₂	409 ^a	0.81	0.025	3.87	1.48	1.93
N ₂	753 ^a	0.92	0.039	5.31	2.71	2.36
CF ₄	552 ^a	1.27	0.177	17.36	19.2	1.31
					3.62×10^5 ,	
CO ₂	734 ^d , 713 ^c	0.98	0.239	30.41	3.52×10^5	0.98

*References: ^aHesse et al. (1996)²⁸; ^bAbraham and Whiting (1990)⁴⁰; ^cRichon and Renon (1980)²⁰; ^dHayduk et al. (1972)¹⁶; ^eKing and Al-Najjar (1977).¹⁹

None of the models in the literature can predict Henry's law constants for light alkanes or rare gases. Meanwhile, the universal prediction method proposed in the present study has significant merit; it satisfactorily predicts Henry's law constants of alkanes at $T_{ri} < 3$ covering a variety of solute-solvent combinations including light alkanes and also rare gases.

Conclusions

Universal methods for the prediction of Henry's law constants (H_i^∞) for alkane/alkane binaries have not been established. The present study established a practical prediction method for the H_i^∞ values of alkane/alkane binaries representing the H_i^∞ data in the literature covering alkane solutes from methane to decane, and alkane solvents from heptane to tetra-cosane at temperatures from 258 to 475 K. The original ideas contained in the present study are summarized as follows.

From Eq. 4 combined with Eqs. 14 to 16, Henry's law constants for alkane/alkane binaries for the temperature ranges from $T_{ri} < 3$ are accurately predicted, where infinite-dilution activity coefficients for simple fluids in alkane solvents are modified as Eq. 14 and hypothetical liquids are defined in terms of the vapor pressures given by Eq. 16 and the fugacity coefficients given by Eq. 15 at temperatures above solute critical. If a pure liquid at the system temperature and at the saturated vapor pressure is chosen as a standard state of activities, the infinite-dilution activity coefficients based on this standard state are convenient for representing solution structures and molecular interactions in alkane/alkane binaries at infinite dilution, where the entropy-enthalpy compensation, $-298.15s_i^{E,\infty}/h_i^{E,\infty} = -1.8$, holds. Conventional models, such as the regular solution, the Flory-Huggins, and the free volume models, fail to accurately predict the partial molar quantities, $s_i^{E,\infty}$ and $h_i^{E,\infty}$ of simple fluids. Of the 42 data sets of the high-pressure VLE data for alkane/alkane binaries in the literature, the nine data sets listed in Table 3 are in the best agreement with those predicted by the present model under dilute conditions, and they are useful for developing a model describing high-pressure VLE. The present model can predict the H_i^∞ values of not only alkanes but also a substance having a smaller or the same acentric factor with an alkane that has the same molecular surface area with the substance, where the measure of the molecular surface area is given by Eq. 27; the present model accurately predicts Henry's law constants for Ar, Kr, Xe, and CCl_4 in hexadecane.

Literature Cited

- Chappelow CC III, Prausnitz JM. Solubilities of gases in high-boiling hydrocarbon solvents. *AIChE J.* 1974;20:1097-1103.
- Rodriguez AT, Patterson D. Prediction of activity coefficients and Henry's constants at infinite dilution for mixtures of *n*-alkanes. *Fluid Phase Equilib.* 1984;17:265-279.
- Kato S, Hoshino D, Noritomi H, Nagahama K. Determination of infinite-dilution partial molar excess entropies and enthalpies from the infinite-dilution activity coefficient data of alkane solutes diluted in longer-chain-alkane solvents. *Ind Eng Chem Res.* 2003;42:4927-4938.
- Prausnitz JM, Shair FH. A thermodynamic correlation of gas solubilities. *AIChE J.* 1961;7:682-687.
- Yen LC, McKetta JJ Jr. A thermodynamic correlation of nonpolar gas solubilities in polar nonassociated liquids. *AIChE J.* 1962;8:501-507.
- Prausnitz JM, Chueh PL. *Computer Calculations for High-Pressure Vapor-Liquid Equilibria*. New York, NY: Prentice-Hall; 1968.
- Pitzer KS. The volumetric and thermodynamic properties of fluids. I.

Theoretical basis and virial coefficients. *J Am Chem Soc.* 1955;77:3427-3433.

- Prausnitz JM. *Molecular Thermodynamics of Fluid-Phase Equilibria*. New York, NY: Prentice-Hall; 1969.
- Reid RC, Prausnitz JM, Poling BE. *The Properties of Gases and Liquids*. New York, NY: McGraw-Hill; 1987.
- Gjaldbaek JC. The solubility of hydrogen, oxygen, and carbon monoxide in some non-polar solvents. *Acta Chem Scand.* 1952;6:623-628.
- Lannung A, Gjaldbaek JC. The solubility of methane in hydrocarbons, alcohols, water, and other solvents. *Acta Chem Scand.* 1960;14:1124-1128.
- Thomsen ES, Gjaldbaek JC. Solubility of cyclopropane in perfluoro-*n*-heptane, *n*-hexane, benzene, dioxane, and water. *Dansk Tidsskrift Farmaci.* 1963;37:9-17.
- Ng S, Harris HG, Prausnitz JM. Henry's constants for methane, ethane, ethylene, propane, and propylene in octadecane, eicosane, and docosane. *J Chem Eng Data.* 1969;14:482-483.
- Lenoir JY, Renault P, Renon H. Gas chromatographic determination of Henry's constants of 12 gases in 19 solvents. *J Chem Eng Data.* 1971;16:340-342.
- Jadot R. Determination of Henry constants by chromatography. *J Chim Phys Phys-Chim Biol.* 1972;69:1036-1040.
- Hayduk W, Walter EB, Simpson P. Solubility of propane and carbon dioxide in heptane, dodecane, and hexadecane. *J Chem Eng Data.* 1972;17:59.
- Hayduk W, Castaneda R. Solubilities of the highly soluble gases, propane, and butane, in normal paraffin and polar solvents. *Can J Chem Eng.* 1973;51:353-348.
- Fleury D, Hayduk W. Solubility of propane in isomers of hexane and other nonpolar solvents. *Can J Chem Eng.* 1975;53:195-199.
- King MB, Al-Najjar H. The solubilities of carbon dioxide, hydrogen sulfide, and propane in some normal alkanes. II. Correlation of data at 25°C in terms of solubility parameters and regular solution theory. *Chem Eng Sci.* 1977;32:1247-1252.
- Richon D, Renon H. Infinite dilution Henry's constants of light hydrocarbons in *n*-hexadecane, *n*-octadecane, and 2,2,4,4,6,8,8-heptamethylnonane by inert gas stripping. *J Chem Eng Data.* 1980;25:59-60.
- Parcher JF, Johnson DM. Methane retention time versus mathematical dead time. *J Chromatogr Sci.* 1980;18:267-272.
- Monfort JP, Arriaga JL. Chromatographic determination with an exponential dilutor of Henry constants of hydrocarbon mixtures. *Chem Eng Commun.* 1980;7:17-25.
- De Ligny CL, Van Houwelingen JC. Correlation and prediction of solubility and standard entropy of solution of gases in liquids by means of analysis of variance and/or principal components analysis. *Fluid Phase Equilib.* 1986;27:263-287.
- Gonzalez R, Murrieta-Guevara F, Parra O, Trejo A. Solubility of propane and butane in mixtures of *n*-alkanes. *Fluid Phase Equilib.* 1987;34:69-81.
- Hayduk W, Asatani H, Miyano Y. Solubilities of propene, butane, isobutane, and isobutene gases in *n*-octane, chlorobenzene, and *n*-butanol solvents. *Can J Chem Eng.* 1988;66:466-473.
- Colson D, Vanhove D. Solubilities of each of several *n*-alkanes in *n*-hexadecane, in 1-chloro-*n*-hexadecane, in *n*-hexadecan-1-ol, and in *n*-eicosane, measured by a dynamic method. *J Chem Thermodyn.* 1990;22:1217-1222.
- Zuliani M, Barreau A, Vidal J, Alessi P, Fermeglia M. Measurements, correlation and prediction of Henry's constants of light alkanes in model heavy hydrocarbons and petroleum fractions. *Fluid Phase Equilib.* 1993;82:141-148.
- Hesse P, Battino JR, Scharlin P, Wilhelm E. Solubility of gases in liquids. 20. Solubility of He, Ne, Ar, Kr, N₂, O₂, CH₄, CF₄, and SF₆ in *n*-alkanes $n\text{-C}_7\text{H}_{2l+2}$ ($6 \leq l \leq 16$) at 298.15 K. *J Chem Eng Data.* 1996;41:195-201.
- Kato S, Hoshino D, Noritomi H, Nagahama K. Prediction of activity coefficients using UNIQUAC interaction parameters correlated with constant-temperature VLE data for alkane/alkane binaries. *Fluid Phase Equilib.* 2004;219:41-47.
- Harvey AH. Semiempirical correlation for Henry's constants over large temperature ranges. *AIChE J.* 1996;42:1491-1494.
- Morgan DL, Kobayashi R. Direct vapor pressure measurements of ten *n*-alkanes in the C₁₀-C₂₈ range. *Fluid Phase Equilib.* 1994;97:211-242.
- King MB, Al-Najjar H. A method for correlating and extending vapor

- pressure data to lower temperatures using thermal data: vapor pressure equations for some *n*-alkanes at temperatures below the normal boiling point. *Chem Eng Sci.* 1974;32:1003-1011.
33. Lyckman EW, Eckert CA, Prausnitz JM. Generalized liquid volumes and solubility parameters for regular solution application. *Chem Eng Sci.* 1965;20:703-706.
34. Yokoyama C, Arai K, Saito S. A semiempirical equation of state for nonpolar and polar substances on the basis of perturbation theory. *J Chem Eng Jpn.* 1982;16:345-352.
35. Elbro HS, Fredenslund A, Rasmussen P. A new equation for the prediction of solvent activities in polymer solutions. *Macromolecules.* 1990;23:4707-4714.
36. Knapp K, Doring K, Oellrich L, Plocker U, Prausnitz JM. Vapor–*Liquid Equilibria for Mixtures of Low Boiling Substances* (Data series). Vol. VI. Frankfurt am Main, Germany: DECHEMA; 1982.
37. Lhotak V, Wichterle I. Vapor–liquid equilibria in the ethane-*n*-butane system at high pressures. *Fluid Phase Equilib.* 1981;6:229-235.
38. Beranek P, Wichterle I. Vapor–liquid equilibria in the propane-*n*-butane system at high pressures. *Fluid Phase Equilib.* 1981;6:279-282.
39. Blanc CJ, Setier JCB. Vapor–liquid equilibria for ethane–propane system at low temperature. *J Chem Eng Data.* 1988;33:111-115.
40. Abraham MH, Whiting GS. Thermodynamics of solute transfer from water to hexadecane. *J Chem Soc Perkin Trans.* 1990;2:291-300.

Manuscript received Oct. 12, 2004, and revision received Apr. 4, 2005.